Received: 27 February 2021 | Revised: 15 June 2021 | Accepted: 16 July 2021

IET Renewable Power Generation

DOI: 10.1049/rpg2.12257

ORIGINAL RESEARCH PAPER

Application of real-time nonlinear model predictive control for wave energy conversion

Ali S. Haider[1] | **Ted K.A. Brekken**[1] | **Alan McCall**[2]

[1] Electrical Engineering and Computer Science, Oregon State University, Corvallis, Oregon, USA

[2] Dehlsen Associates, LLC., Santa Barbara, California, USA

Correspondence
Ali S. Haider, Electrical Engineering and Computer Science, Oregon State University, Corvallis, Oegon, USA.
Email: haidera@oregonstate.edu

Funding information
Office of Energy Efficiency and Renewable Energy, Grant/Award Number: DE-EE0007175

Abstract
This article presents an approach to implement a Nonlinear Model Predictive Controller (NMPC) in real-time with a non-standard cost index. The proposed technique's applications are presented to maximize the energy produced by a Wave Energy Converter (WEC) when the cost index is a non-quadratic piecewise discontinuous functional of some design variables. The presented framework is based on pseudo-quadratisation and weight scheduling, which is implemented using the ACADO toolkit for MATLAB/Simulink. The proposed strategy features code generation and deployment on the real-time target machines for industrial applications. The simulations and experiments confirm the success of the proposed approach in achieving the feasible operation of the NMPC and an optimal power capture by the wave energy converters.

1 | INTRODUCTION

Renewable energy technologies present a viable, sustainable solution to the growing energy demands of the world. The ocean provides a potential for an enormous untapped energy resource [1]. Interest in ocean wave energy has triggered research in the optimal power capture techniques for wave energy converters. Achieving optimal power capture by a WEC is a multifaceted objective. It depends on factors such as the physical design of the WEC, the ocean conditions, and the control techniques. Model Predictive Control (MPC) is a promising control approach for wave energy converters' relatively slow plant dynamics because it maximizes energy capture while respecting the system's mechanical limits [2]. MPC is a look ahead control strategy that predicts future system behaviour to solve a constrained optimization problem and determines the best control action to maximize the output power of a WEC [3]. The MPC algorithm uses an internal model of the plant to predict the future states of the system. Most of the literature formulates the MPC problem by considering linear WEC plant dynamics with a quadratic performance index [4]. Nonlinear MPC design is required if nonlinear or time-varying plant dynamics are addressed, such as nonlinear mooring force and time-varying PTO dynamics [5]. However, most of the research on this subject focuses on formulating some form of standard convex quadratic performance functional for either a linear or nonlinear MPC optimization problem. The primary reason for such a formulation is the availability of efficient algorithms to solve standard convex optimization problems. The execution time becomes a significant concern when the ultimate objective is to solve the optimization problem and deploy the algorithm on real-time target machines to control the PTO mechanisms [6].

An increase in the WEC efficiency requires considering the nonlinear effects in the WEC dynamics and the PTO mechanisms and treating the whole system in an integrated way, that is, the point absorber dynamics, the PTO system, and the control strategy. This results in MPC optimization formulations that have nonconvex and non-standard cost functionals. The capability of an NMPC formulation to handling such non-standard cost indexes is still mostly an unaddressed issue. This issue becomes important during the deployment phase of NMPC in real-time applications; for example, the NMPC designed in [5] does not focus on the real-time applicability of the proposed solution. Nonlinearities in the WEC dynamic models and non-standard cost functions are addressed using pseudo-spectral methods and differential flatness in [7, 8], where the developed nonlinear program is solved by the Sequential Quadratic Programming (SQP) method using Matlab routines fmincon and quadprog. The Economic Model Predictive

Control (EMPC) method is presented in [9, 10], where the concept of a tracking cost function is presented, and the cost function reflects the economic objective of the system. Pseudo-spectral methods and EMPC techniques are promising solutions but are computationally intensive for nonlinear MIMO systems with non-standard optimization objectives, especially if the end objective is deploying the proposed algorithm to an embedded controller using the available Real-Time Iterative (RTI) solvers.

This research presents a framework to implement NMPC in real-time for multiple degrees of freedom wave energy converters formulated as general time-varying nonlinear dynamic systems. It also considers the problems in which the PTO mechanisms' cost index takes non-standard forms, such as affine form, polynomial with a degree higher than two, piecewise polynomial of PTO force, trigonometric polynomials of design variables, and time-varying parametric. This work focuses on practical implementation considerations rather than in-depth mathematical formulation or algorithm design, for instance, the reformulation of a given non-standard NMPC problem for implementation on a real-time target-machine using a nonlinear optimization solver, such as ACADO, which supports differential-algebraic process dynamics and constraints [11, 12]. This paper explores the pseudo-quadratisation technique to reformulate the non-quadratic objection functional to quadratic-like forms. This technique enables the use of available software package for the problem sets that have non-standard cost indexes.

Moreover, the technique of weight scheduling is presented to broaden the application of the proposed technique further to include the problems that require the optimization of cost indexes defined in a piecewise polynomial form. Such systems are common in the wave energy generation sector. The proposed method is applied to case study NMPC optimal power take-off (PTO) problems that take the form of a real-time optimization problem over a non-standard piecewise polynomial cost index.

2 | MATHEMATICAL FORMULATION FOR NMPC

A given NMPC problem optimizes a manipulated variable $u \subseteq w$ to maximize some cost functional P of a set of design variables w, while respecting the given system constraints. This research focuses on a class of NMPC problems in which the cost functional takes on a general nonlinear piecewise polynomial form. Considering the case of finite-horizon optimization, we can mathematically describe the NMPC problem of such a class as:

$$\max_{\mathbf{u}} P\left(\mathbf{w}\right) = \begin{cases} P_1\left(\mathbf{w}\right) + \rho_{N,1}\left(\mathbf{w}\right) w_n < R_1 \\ P_2\left(\mathbf{w}\right) + \rho_{N,2}\left(\mathbf{w}\right) R_1 \leq w_n \leq R_2 \\ \vdots \qquad\qquad \vdots \\ P_j\left(\mathbf{w}\right) + \rho_{N,j}\left(\mathbf{w}\right) R_{j-1} \leq w_n \leq R_j \end{cases} \tag{1}$$

subject to,

$$\ddot{\mathbf{x}} = g\left(\mathbf{w}\right) \tag{2}$$

$$q = p\left(\mathbf{w}\right) \tag{3}$$

$$\mathrm{Y}_1 = \mathbf{B}_{\mathbf{equal}} \tag{4}$$

$$\mathbf{B}_{\mathbf{lower}} \leq \mathrm{Y}_2 \leq \mathbf{B}_{\mathbf{upper}} \tag{5}$$

where Y_{i} vectors are of the following forms,

$$\begin{aligned} \mathrm{Y}_1 &= \mathbf{\Psi}_1 \mathbf{q}, \\ \mathrm{Y}_2 &= \mathbf{\Psi}_2 \mathbf{q} \end{aligned} \tag{6}$$

here, **g** and **p** are vectors of real-valued nonlinear functions of some design variables **w**, and P_i and $\rho_{N,j}$ are real-valued polynomial functions of **w**. The real-valued design variable $w_n \in \mathbf{w}$ is responsible for the switching of the cost manifold in (1) depending upon its magnitude lying in a particular interval defined by some real numbers R_i. The description of various variables and constants in (1) through (6) is given in Table. 1. The maximization of the cost functional in Equation (1) is subjected to the dynamic constraints in Equation (2), which corresponds to a general nonlinear state-space description of the physical WEC plant. The proposed NMPC formulation considers the nonlinear algebraic constraints described by Equation (3). The equality and inequality constraints are described by Equations (4) and (5), respectively. These constraints are formulated in Equation (6) in terms of the algebraic expressions of the design variables.

3 | TIME DOMAIN MODEL OF A WEC

Consider a single degree of freedom heaving point absorber WEC with a linear generator PTO mechanism, as shown in Figure 1: a single input multiple output system with heave PTO force as the control input and the velocity and positions of the float as outputs. The time-domain model of a WEC with frequency-dependent damping has been developed and validated in [13, 14],

$$\mathbf{x} = \left[v_{pto}\ z_{pto}\ F_r\ F \right]^T$$

$$\mathbf{g} = \begin{bmatrix} \dfrac{-k}{M} z_{pto} + \dfrac{1}{M} F_r + \dfrac{1}{M} u + \dfrac{1}{M} d \\ v_{pto} \\ -c_a v_{pto} - c_b z_{pto} - c_d F_r - c_e F \\ F_r \end{bmatrix} \tag{7}$$

The description of various variables and constants in Equation (7) is given in Table 1. The state-space form of the WEC dynamics in Equation (7) becomes the differential

TABLE 1 Notations

Variable	Description
$\mathbf{w}$	Set of design variables
N	Prediction horizon
$x \subseteq w$	State vector
$u \subseteq w$	Manipulated variable
$\rho_{N,i}$	Finite horizon terminal cost penalty
P_i	Real-valued polynomial of design variables
$\mathbf{\Psi_i}$	Constant matrices
$\mathbf{B_i}$	Constant column vectors
$\mathbf{Y_i}$	Column vectors of real-valued nonlinear functions
$\mathbf{q}$	Column vectors of real-valued nonlinear functions
R_i	Some real number
V_{pto}	Float heave velocity (m/s)
Z_{pto}	Float heave position (m)
F_r	Radiation force (N)
F	Time integral of the radiation force
u	Control input, F_{pto}(N)
m	Float mass (kg)
A	Float added mass (kg)
k	Float hydrostatic stiffness (N/m)
C_i	Constants with $i,j \in$E $\{a, b\}$
d	Excitation force disturbance, F_e (N)
I_{pto}	PTO generator current
M	Effective mass $m + A\ (\infty)$ (Kg)
$\mathbf{h}$	Column vectors of real-valued nonlinear functions
$\mathbf{h_N}$	Column vectors of real-valued nonlinear functions

constraints in Equation (2). The dynamic system (7) may include time-dependent variables to incorporates some practical scenarios, such as a change in the configuration of float [14] or actively varying the number of PTO generator pickup coils.

3.1 | Nonquadratic WEC-PTO models

The electrical power output from the PTO mechanism of the WEC is the difference between the mechanical power input from the waves and the losses in the PTO system. For a given PTO generator with a converter efficiency η_{Conv}, the copper loss constant K_{Cu}, and the winding resistance R_Ω, the electrical power cost functional to be maximized, including the electrical losses, is given by,

$$\max_{F_{pto}} P_E = \eta_{Conv}\left(F_{pto}v_{pto} - K_{Cu}I_{pto}^2R_\Omega\right) \tag{8}$$

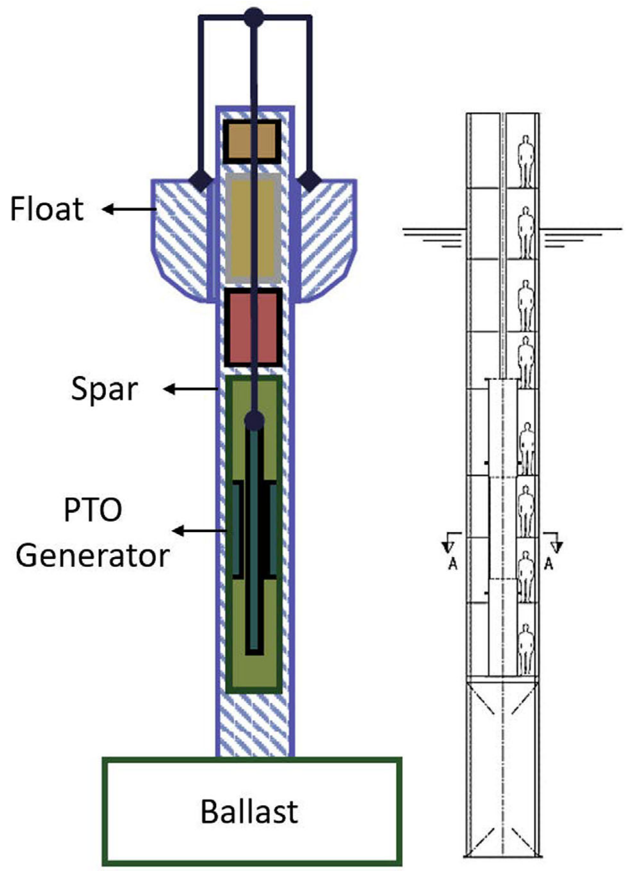

FIGURE 1 Point absorber WEC with linear generator PTO mechanism by Wedge-Global

3.1.1 | Higher-order PTO models

This case study scenario is taken from McCleer Power's Linear PTO generator with the PTO force-current characteristics given by Figure 2. This relation is described by a third-order curve fit between the PTO current and the PTO force,

$$I_{pto}\ \left(F_{pto}\right) = a_3\ F_{pto}{}^3 + a_2F_{pto}{}^2 + a_1F_{pto} + a_0 \tag{9}$$

Putting Equation (9) in Equation (8), we get,

$$\begin{aligned} P_E = c_0F_{pto}v_{pto} - (c_1F_{pto}^6 + c_2F_{pto}^5 + c_3F_{pto}^4 \\ + c_4F_{pto}^3 + c_5F_{pto}^2 + c_6F_{pto} + c_7) \end{aligned} \tag{10}$$

It can be seen that Equation (10) is a higher-order nonquadratic cost functional to be maximized.

3.1.2 | Piecewise linear PTO models

This case study scenario considers the data from Figure 2. However, the relation between the PTO current and the PTO force

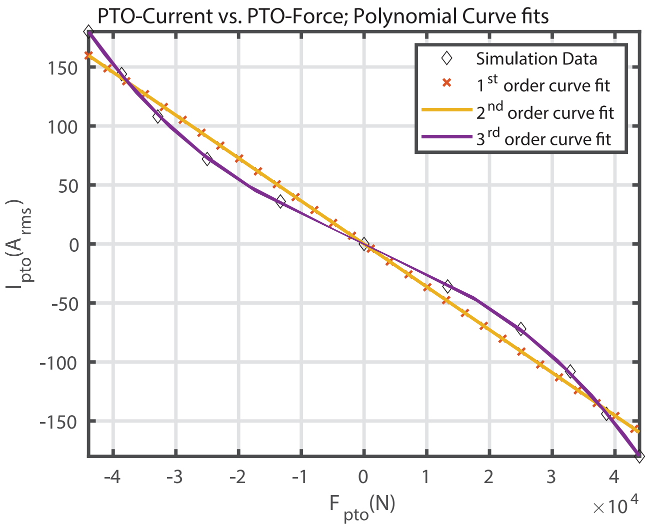

FIGURE 2 Higher-order current-force relation for a WEC PTO generator

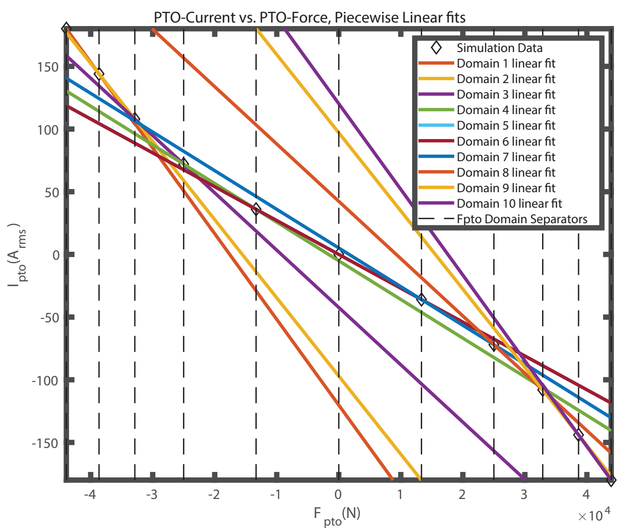

FIGURE 3 Piecewise linear current-force relation for a WEC PTO generator

is approximated by the piecewise linear curves that fit between each of the two consecutive data points in Figure 3. Each linear curve fit is valid for the corresponding domain of the PTO force. For Figure 3, these piecewise linear curve fits are described by Equation (11).

$$I_{pto}\left(F_{pto}\right)=\begin{cases} a_{11}F_{pto}+a_{10} & F_{k1}\le F_{pto}<F_{k2}\\ a_{21}F_{pto}+a_{20} & F_{k2}\le F_{pto}<F_{k3}\\ a_{31}F_{pto}+a_{30} & F_{k3}\le F_{pto}<F_{k4}\\ \vdots & \vdots\\ a_{101}F_{pto}+a_{100} & F_{k10}\le F_{pto}<F_{k11}\end{cases} \tag{11}$$

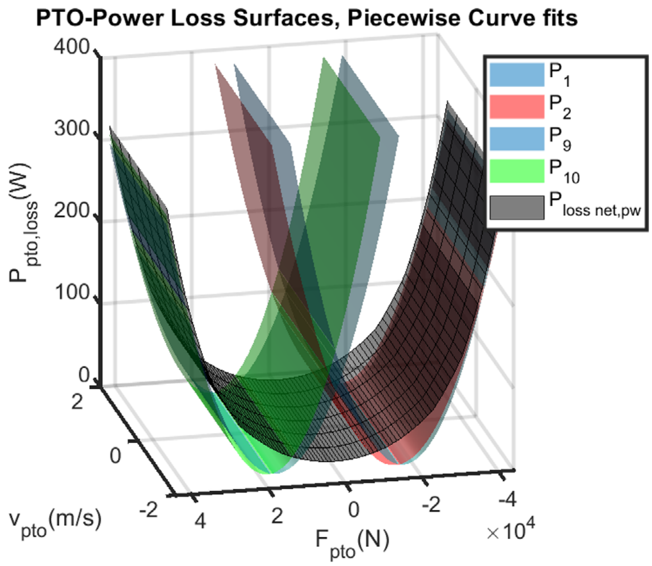

FIGURE 4 WEC-PTO power loss manifolds for piecewise linear curve fitting (only a few surfaces are shown for clarity)

Putting Equation (11) in Equation (8), we get,

$$P_{E,i}=c_0\ F_{pto}v_{pto}-\left(c_{i1}F_{pto}^2+c_{i2}F_{pto}+c_{i3}\right), \quad i\in\{1,2\ldots 10\} \tag{12}$$

It can be seen that Equation (12) is a piecewise quadratic cost functional to be maximized. Comparing Equation (8) with Equation (12), we can observe that the power loss component of P_E in Equation (12) is dependent upon the magnitude of PTO force. Each component represents a manifold, which is a 2D surface, as shown by Figure 4.

3.1.3 | Piecewise nonlinear PTO models

This case study scenario is taken from Wedge Global's linear PTO generator with the PTO force-current characteristics given by Figure 5. This relation is approximated by piecewise nonlinear curve fits over the PTO force domains. For Figure 5, these piecewise curve fits are described by Equation (13).

$$I_{pto}\left(F_{pto}\right)=\begin{cases}\dfrac{F_{pto}-\alpha}{\beta} & F_{pto}\le -F_k\\ -\sqrt{\dfrac{-F_{pto}}{\gamma}} & -F_k<F_{pto}<0\\ \sqrt{\dfrac{F_{pto}}{\gamma}} & 0\le F_{pto}<F_k\\ \dfrac{F_{pto}+\alpha}{\beta} & F_{pto}\ge F_k\end{cases} \tag{13}$$

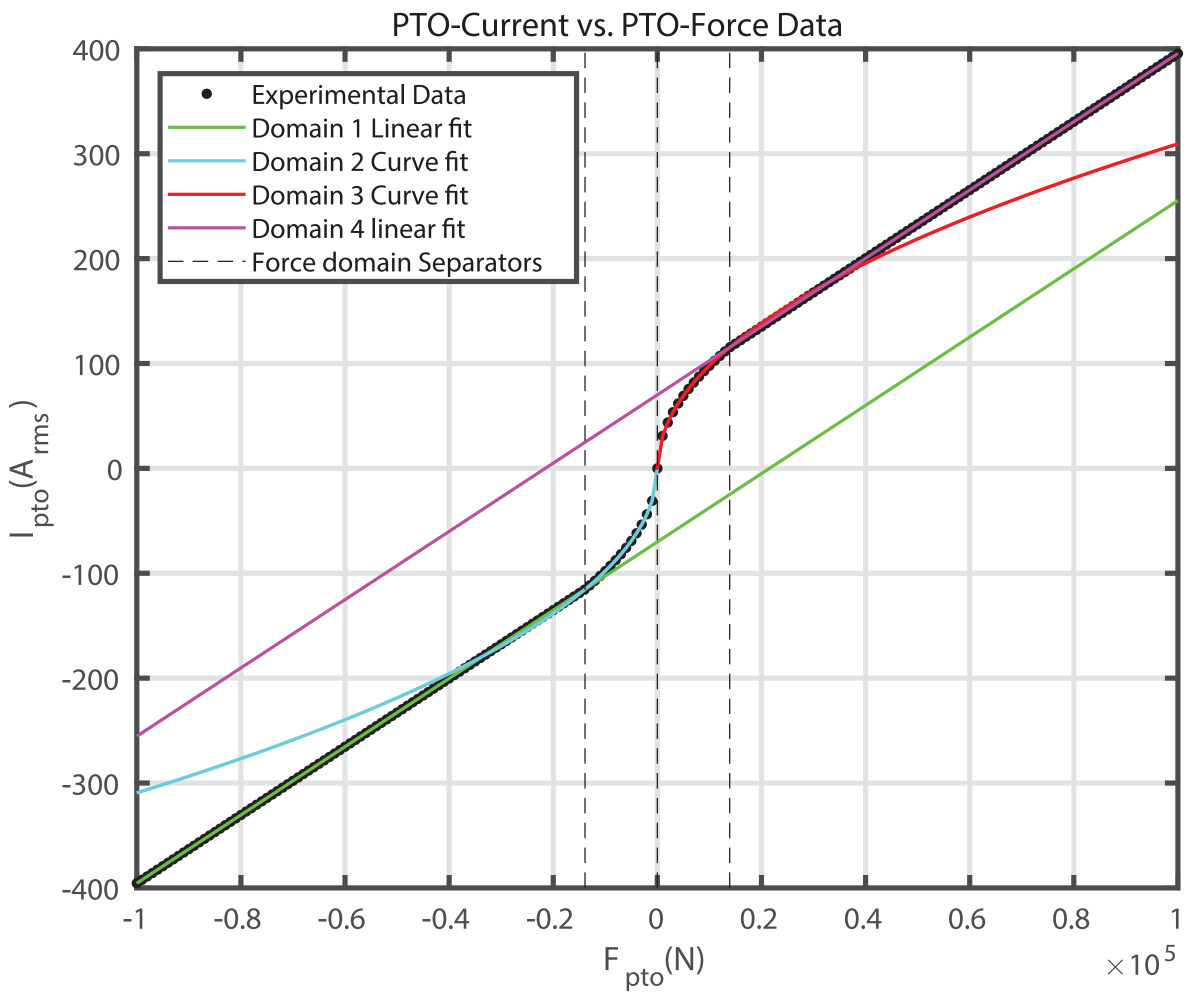

FIGURE 5 Piecewise nonlinear current-force relation for a WEC PTO generator

Putting Equation (13) in Equation (8), we get Equation (14). It can be seen that Equation (14) is a higher-order piecewise non-quadratic cost functional to be maximized. Comparing Equation (14) with Equation (8), we can observe that the power loss component of P_E in Equation (14) is dependent upon the magnitude of PTO force. Each component represents a manifold, which is a 2D surface, similar to Figure 4.

$$P_E = \begin{cases} c_{10}F_{pto}v_{pto} + c_{11}F_{pto}^2 v_{pto} - c_{12}F_{pto}^2 + c_{13}F_{pto} + c_{14}v_{pto} - c_{15} & F_{pto} \leq -F_k \\ c_{20}F_{pto}v_{pto} + c_{21}F_{pto} & -F_k < F_{pto} < 0 \\ c_{30}F_{pto}v_{pto} - c_{21}F_{pto} & 0 \leq F_{pto} < F_k \\ c_{40}F_{pto}v_{pto} + c_{11}F_{pto}^2 v_{pto} - c_{12}F_{pto}^2 - c_{13}F_{pto} + c_{14}v_{pto} - c_{15} & F_{pto} \geq F_k \end{cases} \tag{14}$$

4 | NMPC IMPLEMENTATION METHOD

The cost functionals in Equations (10), (12), and (14) are not standard quadratic forms. To implement such problems, we have used the method of pseudo-quadratisation and weight scheduling. With this technique, we can extend the capabilities of the standard quadratic solvers [11] to implement the NMPC for the non-standard optimization problems according to the scheme shown in Figure 6.

4.1 | Pseudo-quadratisation and weight scheduling

If the cost functional P in (1) is not quadratic, then the technique of pseudo-quadratisation relies on appropriately defining two vectors of nonlinear real-valued functions, $h(\mathbf{w})$ and $h_N(\mathbf{w})$ to convert P into quadratic-like forms. A proper selection of these vectors along with the weighting matrices W_i would enable us to put Equation (1) into a form given by Equation (15).

$$\begin{aligned} P_i(\mathbf{w}) &= \frac{1}{2}\mathbf{h}^{\mathbf{T}} W_i \mathbf{h}, \quad i = 1, 2 \ldots, j \\ \rho_{N,i}(\mathbf{w}) &= \frac{1}{2}\mathbf{h}_{\mathbf{N}}^{\mathbf{T}} W_{N,i} \mathbf{h}_{\mathrm{N}}, \; i = 1, 2 \ldots, j \end{aligned} \tag{15}$$

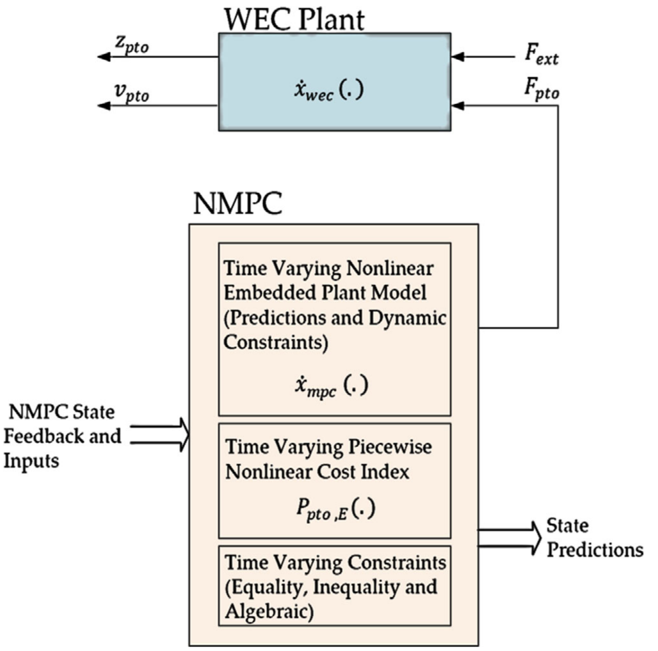

FIGURE 6 Implementing nonlinear MPC with ACADO Toolkit

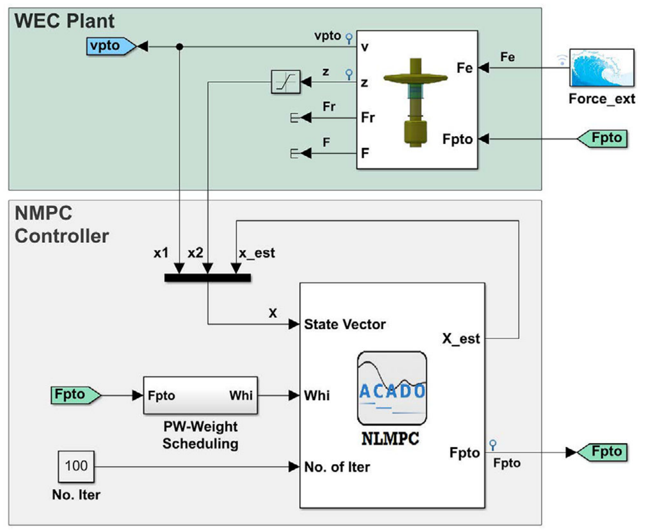

FIGURE 7 NMPC implementation in Simulink using ACADO Toolkit

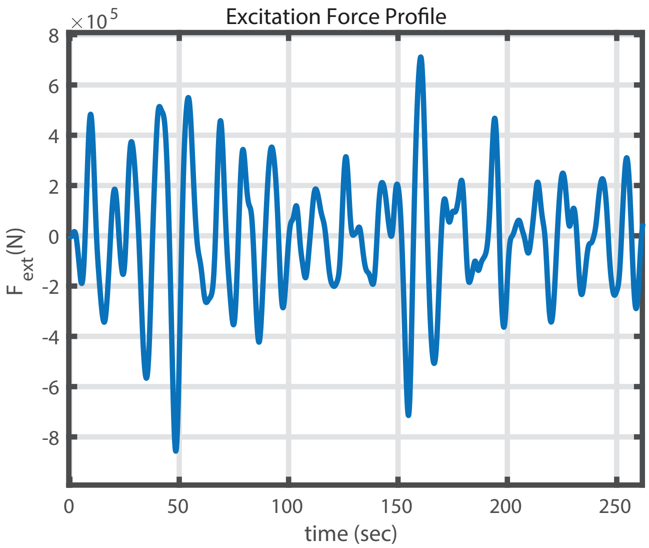

FIGURE 8 Excitation force profile for simulation of the proposed controller

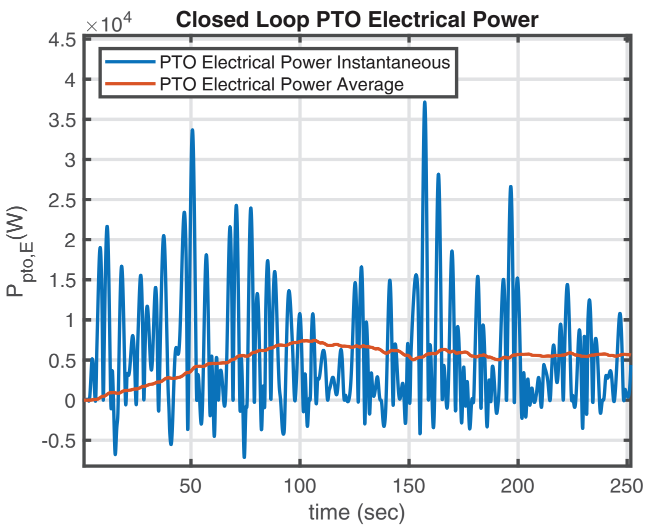

FIGURE 9 Instantaneous and average PTO power output

The expression in Equation (15) resembles a quadratic form but might not expand to a quadratic polynomial of design variables, as we will discuss shortly; hence, they are named pseudo-quadratic forms. For nonconvex problems, the convex relaxation of the cost manifold P_i in Equation (15) can be implemented by the superposition of some convexifying manifold D_i. Let us denote the modified manifold as $P_{i,m}$ and we can write it as:

$$P_{i,m}\ (\mathbf{w}) = \frac{1}{2}\ \mathbf{h}^{\mathbf{T}} W_i h + D_i\ (\mathbf{w}) \tag{16}$$

The manifold D_i can be decomposed into the quadratic form using appropriate weighting matrices $W_{d,i}$,

$$D_i\ (\mathbf{w}) = \frac{1}{2}\ \mathbf{h}^{\mathbf{T}} W_{d,i} h \tag{17}$$

Using Equation (17) in Equation (16), the modified manifold $P_{i,m}$ can be expressed as:

$$P_{i,m}\ (\mathbf{w}) = \frac{1}{2}\ \mathbf{h}^{\mathbf{T}} \left(W_i + W_{d,i}\right) h\ = \frac{1}{2}\ \mathbf{h}^{\mathbf{T}} W_{i,m} h \tag{18}$$

The choice of D_i and hence, the weighting matrices $W_{d,i}$ are not unique and depend upon a specific cost functional Equation (15) for a given problem. The manifold D_i can be used to appropriately increase the weights of the convex terms

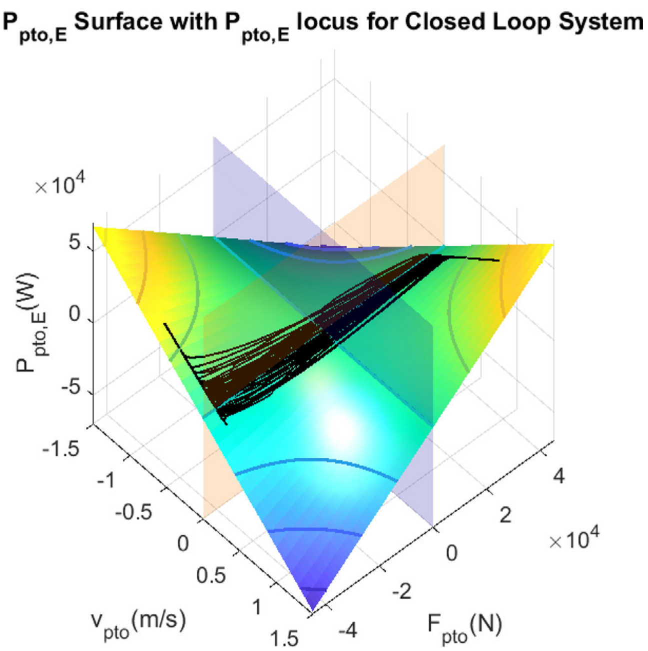

FIGURE 10 The PTO force and PTO velocity locus on the WEC electrical power cost functional

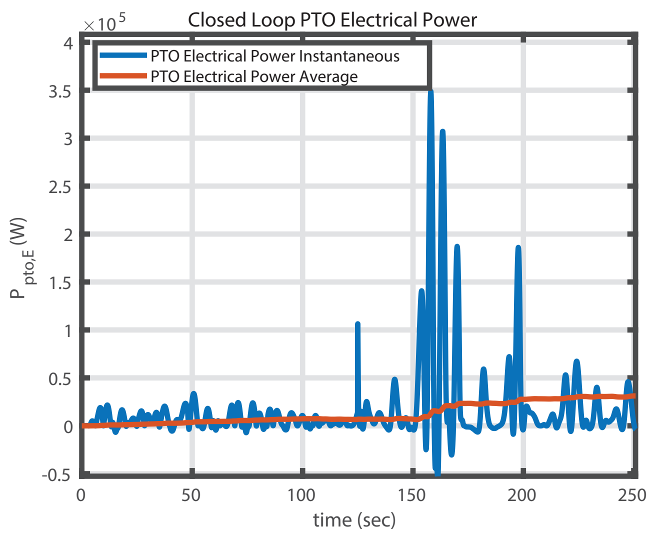

FIGURE 11 Instantaneous and average PTO power output for piecewise nonlinear cost manifold

of P_i in Equation (15), for example F^n_{pto}, where n is an even number. Some other deciding factors are the convergence rate of the optimization algorithm and the modified cost manifold's allowed deviation in Equation (18) from the actual cost manifold (1).

Now let us apply the above technique to the higher-order PTO model in Equation (10). Defining a $\mathbf{h}$ vector as:

$$h = \left[F^3_{pto}\ F^2_{pto}\ F_{pto}\ v_{pto}\ 1\right]^T \tag{19}$$

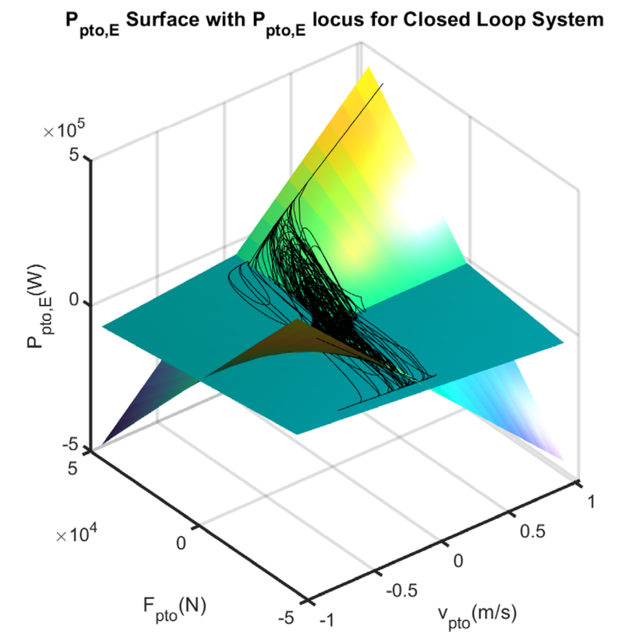

FIGURE 12 The PTO force-velocity locus on piecewise nonlinear cost manifold

Although Equation (10) is not a quadratic form but using Equation (20) in Equation (10), we get a pseudo-quadratic form described by Equation (21).

$$P_E = \frac{1}{2}\,\mathbf{h}^{\mathbf{T}}\left(2\begin{bmatrix} -c_1 & \frac{-c_2}{2} & 0 & 0 & 0 \\ \frac{-c_2}{2} & -c_3 & \frac{-c_4}{2} & 0 & 0 \\ 0 & \frac{-c_4}{2} & -c_5 & \frac{c_0}{2} & \frac{-c_6}{2} \\ 0 & 0 & \frac{c_0}{2} & 0 & 0 \\ 0 & 0 & \frac{-c_6}{2} & 0 & -c_7 \end{bmatrix}\right)h \tag{20}$$

The cost functional expression in Equation (21) can be implemented using nonlinear optimization solver ACADO. Similarly, defining a vector $\mathbf{h}$ for Equation (12) as,

$$h = \left[F_{pto} \quad v_{pto} \quad 1\right] \tag{21}$$

Using Equation (22) in Equation (12), we get a weight-scheduled quadratic form described by Equation (23).

$$P_{E,i} = \frac{1}{2}\,\mathbf{h}^{\mathbf{T}}\left(2\begin{bmatrix} -c_{i1} & \frac{c_0}{2} & \frac{-c_{i2}}{2} \\ \frac{c_0}{2} & 0 & 0 \\ \frac{-c_{i2}}{2} & 0 & -c_{i3} \end{bmatrix}\right)h \tag{22}$$

The cost functional expression in Equation (23) can be implemented using nonlinear optimization solver ACADO using weight scheduling for the PTO force.

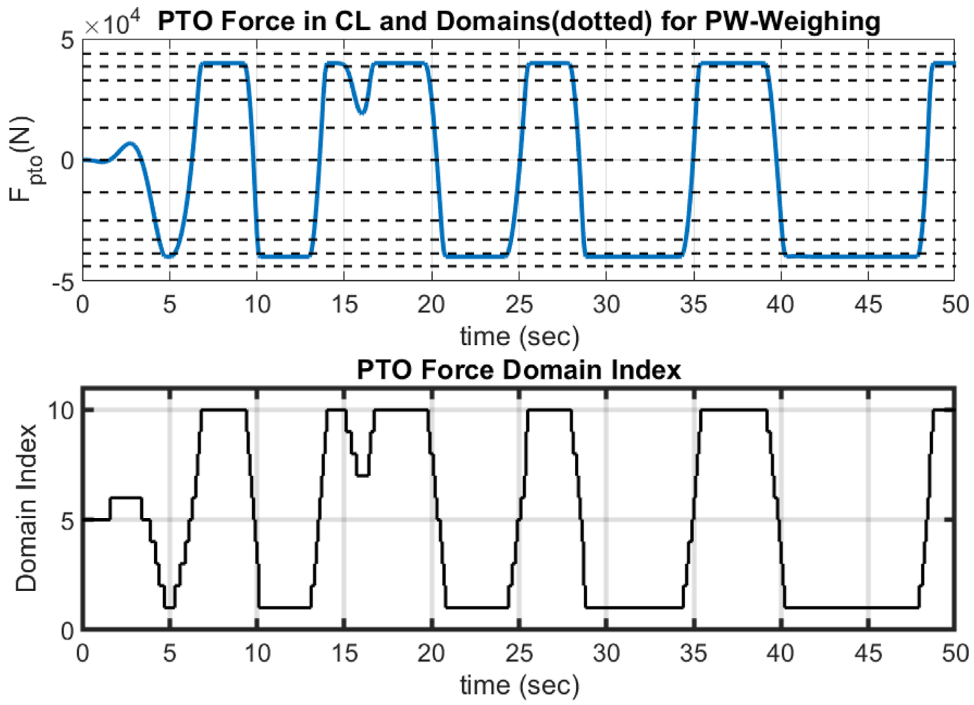

FIGURE 13 The PTO force domains and selection of weight matrix index for cost functional

5 | SIMULATION, TESTING, AND RESULTS

The Simulink block diagram for the implementation of NMPC is shown in Figure 7 for the WEC in Equation (7) using parameter values from [13] and the cost functional in Equation (21). The test excitation force profile is shown in Figure 8, corresponding to a JONSWAP spectrum (significant wave height of 2.5 m, and peak period of 8 s). The plots for the instantaneous PTO power and the average PTO power are shown in Figure 9. The NMPC optimization solution is convergent, and the locus of the PTO force and the PTO velocity along with the manifold (21) are shown in Figure 10. The planes separating the four quadrants of the PTO velocity and force are also shown in Figure 10. The locus traverses a trajectory that lies on the manifold Equation (21), satisfying the cost objective. The trajectories are also inclined towards the first and fourth octant of the PTO force-velocity space as the controller attempts to actuate the WEC PTO generator to make the PTO force in-phase with the PTO velocity to maximize the PTO power capture.

For the piecewise cost functional of the form (23), the plots for the instantaneous PTO power and the average PTO power are shown in Figure 11. For an illustration of piecewise case Equation (23), a PTO cost manifold with only two pieces is considered, as shown in Figure 12. The controller is manually switched from one cost manifold to the other at 150 s. The locus of the PTO force and the PTO velocity, along with the cost manifolds, are shown in Figure 12. The locus traverses a trajectory that lies on the manifolds and satisfies the cost objective. In the actual scenarios, the manifold switching would depend upon the current magnitude of PTO force according to Equation (11), as shown in Figure 13. The selection of the weight matrix in Equation (15) would depend on the domain interval of the PTO force at any given time. The QP optimization algorithm withstands the manifold switching operation in Figure 12 and converges to an optimal solution. However, with the ACADO toolkit, there is no theoretical guarantee that the optimization routine can always remain safely in its region of convergence [13]. Given that the cost index formulation in Equation (8) includes a convexifying power loss term, for example the power loss surface plots in Figure 4, and I_{pto} linear curve fits in Figure 3 do not have jump discontinuity at the switching value, the close loop system tends to maintain a stable operation. If the QP problem formulated at a given sample interval is infeasible, the controller will fail to find a solution. This issue can be handled by monitoring the status of the QP solver during each sampling interval and selecting a suboptimal solution when the QP solver fails.

The proposed design is implemented on Speedgoat Performance real-time target machine-109100 [15] with Intel Core i3-3220, 3.3 GHz processor, and 2048 MB of installed RAM. Given the typical ocean wave period of 10 s, a sample time of 0.1 s was selected for the real-time simulation of NMPC. The Speedgoat based controller implementation is shown in Figure 14. The target machine is configured to communicate with the WEC plant over the Modbus TCP/IP channel. The WEC dynamics were emulated on another real-time machine, as shown in Figure 15. An average of 12% processor load was observed per sampling interval during testing. The real-time implementation of the controller confirmed the simulation results. The updated code has been made publicly available

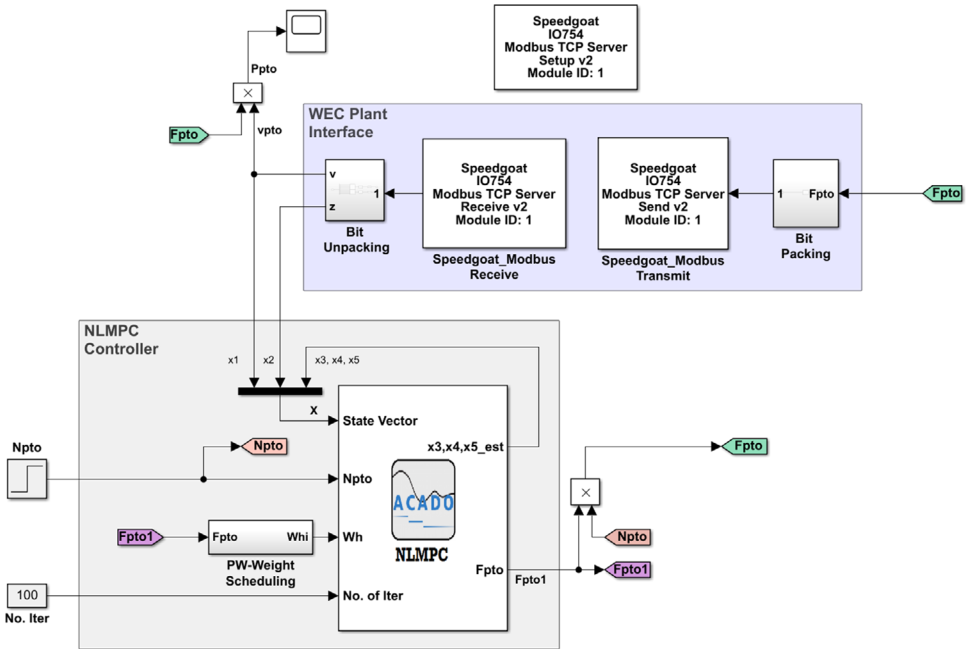

FIGURE 14 Implementation of the proposed NMPC for the Speedgoat real-time target machine

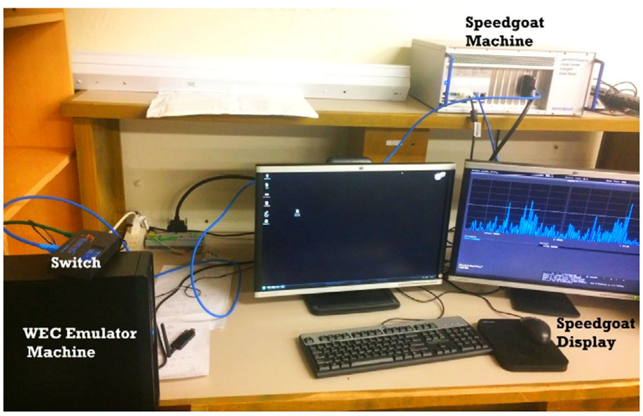

FIGURE 15 Testing the controller using real time target machine and the WEC emulator machine

at the following online repository (github.com/aliSHaider/NMPC_Acado_Simulink_Speedgoat).

6 | CONCLUSION

An approach to implement a Nonlinear Model Predictive Controller (NMPC) in real-time with a non-standard cost index is presented. The case study WEC PTO models were presented. The specific PTO power formulations are non-quadratic piecewise functional of the PTO force and PTO velocity. The method of pseudo-quadratisation and weight-scheduling is used to implement the NMPC problem using the ACADO toolkit for MATLAB/Simulink. The proposed strategy supports code generation, and the controller was deployed on the Speedgoat Performance real-time target machine-109100, coupled to the real-time WEC emulator machine over the Modbus TCP/IP channel. The proposed methodology successfully maintained an overall feasible operation of the real-time NMPC problem in simulation as indicated by the status port of the NMPC QP-solver. The experimental implementation on the Speedgoat target machine confirmed the optimal power capture results from the simulation with an average of 12% processor load.

ACKNOWLEDGEMENTS

This work was funded by the U.S. Department of Energy's Energy Efficiency and Renewable Energy (EERE) office within the Water Power Technologies Office under contract DE-EE0007175. Authors would like to thank Dehlsen Associates, Wedge-Global, and McCleer Power for their technical support and for providing the experimental data.

ORCID

Ali S. Haider https://orcid.org/0000-0002-4651-3157

REFERENCES

1. Muetze, A., Vining, J.G.: Ocean wave energy conversion - a survey. In: Conference Record of the 2006 IEEE Industry Applications Conference Forty-First IAS Annual Meeting, Tampa, Florida, pp. 1410–1417 (2006)
2. Brekken, T.K.A.: On model predictive control for a point absorber wave energy converter. In: 2011 IEEE Trondheim PowerTech, Trondheim, Norway, pp. 1–8 (2011)
3. Richter, M., et al.: Power optimisation of a point absorber wave energy converter by means of linear model predictive control. IET Renewable Power Gener. 8(2), 203–215 (2014)
4. Starrett, M., et al.: Increasing power capture from multibody wave energy conversion systems using model predictive control. In: 2015 IEEE Conference on Technologies for Sustainability (SusTech), Ogden, Utah, pp. 20–26 (2015)

5. Richter, M., et al.: Nonlinear model predictive control of a point absorber wave energy converter. IEEE Trans. Sustainable Energy 4(1), 118–126 (2013)
6. Haider, A.S., Brekken, T.K.A., McCall, A.: A state-of-the-art strategy to implement nonlinear model predictive controller with non-quadratic piecewise discontinuous cost index for ocean wave energy systems. In: 2020 IEEE Energy Conversion Congress and Exposition (ECCE), Detroit, Michigan, pp. 1873–1878 (2020)
7. Li, G.: Nonlinear model predictive control of a wave energy converter based on differential flatness parameterisation. Int. J. Control 90(1), 68–77 (2017)
8. Bacelli, G., Genest, R., Ringwood, J.V.: Nonlinear control of flap-type wave energy converter with a non-ideal power take-off system. Ann. Rev. Control 40, 116–126 (2015)
9. Jia, Y., et al.: Economic model predictive control of a point absorber wave energy converter. IEEE Trans. Sustainable Energy 12(1), 578–586 (2021)
10. Angeli, D., Amrit, R., Rawlings, J.B.: On average performance and stability of economic model predictive control. IEEE Trans. Autom. Control 57(7), 1615–1626 (2012)
11. Quirynen, R., et al.: Autogenerating microsecond solvers for nonlinear MPC: A tutorial using ACADO integrators. Optim. Control. Appl. Methods 36(5), 685–704 (2015)
12. Houska, B., Ferreau, H.J., Diehl, M.: ACADO toolkit—An open-source framework for automatic control and dynamic optimization. Optim. Control. Appl. Methods 32(3), 298–312 (2011)
13. Starrett, M., et al.: Development of a state space model for wave energy conversion systems. In: 2015 IEEE Power Energy Society General Meeting, Denver, Colorado, pp. 1–5 (2015)
14. Marine and Hydrokinetic Data Repository (MHKDR). https://mhkdr.openei.org/, accessed May 14, 2021
15. Speedgoat - The Quickest Path to Real-Time Simulation and Testing. https://www.speedgoat.com/, accessed February 2, 2021

How to cite this article: Haider, A.S., Brekken, T.K.A., McCall, A.: Application of realtime nonlinear model predictive control for wave energy conversion. IET Renew. Power Gener., 15, 3331–3340 (2021). https://doi.org/10.1049/rpg2.12257